ROBUST OPTIMIZATION TECHNIQUES AND DESIGN OF LI-ION BATTERIES

BY

FOLARIN BABAJIDE LATINWO

THESIS

Submitted in partial fulfillment of the requirements
for the degree of Master of Science in Chemical Engineering
in the Graduate College of the
University of Illinois at Urbana-Champaign, 2011

Urbana, Illinois

Advisor:

Professor Richard D. Braatz

ABSTRACT

This thesis applies robust optimization techniques to the design of Lithium-ion batteries with spatially varying porosities. The microstructure of a porous electrode was designed to minimize the Ohmic resistance. The spatial variation in the porosities was found to provide enhanced robustness of the Li-ion battery to uncertainties. This thesis also proposes a robust optimization formulation based on polynomial chaos expansion that is applied in the design of the Li-ion battery and a batch crystallization process. The proposed approach yields an analytic expression for the computation of the variance in the optimization objective that is cheap to evaluate computationally. The estimates of the variance incorporated into the multiobjective optimization were found to be accurate enough for the purposes of robust optimal design.

ACKNOWLEDGEMENTS

The author wishes to express sincere gratitude to Prof. Braatz throughout this process. In addition, special thanks to Professors Schroeder and Kenis for their support in completing this work. And finally, thanks to my friends and family for kind words that carried me through in earning my Master's Degree.

TABLE OF CONTENTS

CHAPTER 1: INTRODUCTION

Lithium-ion batteries with a wide range of sizes and power ratings are becoming increasingly ubiquitous in applications, from implantable cardiovascular defibrillators operating at 10 μA to current hybrid vehicles operating at 100A. At the largest scale, Li-ion batteries are one of the main candidates for the grid storage of energy produced by wind power and other intermittent green power generators. For Li-ion batteries to be the best long-term solution for many of these applications requires substantial improvements in battery performance. Most of the efforts to improve battery performance have focused on developing new chemistries for the electrodes and electrolytes. Another method for performance enhancement is to employ optimal model-based design methods, which can be applied to batteries irrespective of their chemistries. While many recent papers have explored optimal model-based battery design, the effective of uncertainties in the model parameters have not been incorporated into the optimizations.

This thesis was motivated by two observations. First, it is well-established in the literature that uncertainties in external factors such as cost data and internal model parameters such as associated with kinetics and transport can have a very large effect on product quality for batch, semibatch, and continuous manufacturing processes. Second, Li-ion battery operations are a very highly nonlinear dependence on its design parameters, so that the effects of uncertainties on performance cannot be estimated reliably except by employing careful model-based quantification. Quantitative estimates of the effects of uncertainties can be used to decide which model parameters need to be identified with higher accuracy, or to implement optimal designs that are robust to a given level of model uncertainty.

Robust optimal control techniques have been applied to many batch and semi-batch processes including many materials and electrochemical systems and the processes used to manufacture materials. This thesis is the first to apply robust design techniques to a lithium-ion battery. The effect of uncertainties on a performance objective, in this case Ohmic resistance, is quantified. This thesis also applies polynomial chaos expansions to approximate a lithium-ion battery model with simpler algebraic expressions. The motivation for this approximation is the reduction in the computational expense when applying robust optimization. This thesis is the first time that robust optimization techniques have been applied to determine spatially varying microstructure in the design of Li-ion batteries.

This thesis also proposes a new mathematical formulation for robust optimal design. The approach is based on employing a polynomial chaos expansion (PCE) not only in the uncertain model parameters *but also in the design variables*. Because the variance can be analytically computed once the coefficients of the PCE are known, this approach greatly reduces the computational cost of robust optimization.[1]

The thesis is organized as follows. First, previous research in robustness analysis, robust design, optimal design, and polynomial chaos expansions is reviewed. Applications are mentioned from the crystallization of semiconductors and organic molecules to atmospheric aerosols to Lithium-ion batteries. Next robust optimization techniques with an emphasis on distributional robustness analysis are presented. This is followed by a chapter describing uncertainty analysis using polynomial chaos expansions. Then polynomial chaos expansions techniques are applied to the model equations for Li-ion batteries. Following this, the novel approach is applied to a well-

[1] Higher order moments may also be computed from the coefficients of the PCE.

studied crystallization problem and to the design of Li-ion batteries. Finally, the results of the thesis are summarized followed by ideas for future research.

CHAPTER 2: LITERATURE REVIEW

The performance of processes or products can be substantially improved by implementing optimal design or control policies. In practice model uncertainties are significant and can eliminate the improved performance obtainable from optimization. This observation has motivated the development of *robust* optimal design and control methods that ensure improved performance in the presence of uncertainties. Applying robust optimization techniques can be prohibitively computationally expensive when using classical Monte Carlo methods to perform the uncertainty analysis. Distributional robustness analysis techniques have been developed that greatly reduce the computational cost of robustness analysis. Polynomial chaos expansions (PCEs) represent the model outputs as simple algebraic expressions in the uncertain parameters, which further reduces the computational cost of implementing robust optimization. PCEs and related techniques make robust optimization a much more computationally tractable problem.

Optimal control techniques have been applied in a broad range of applications. Gunawan et al. [1] employed optimal control to study rapid thermal annealing for the formation of ultrashallow junctions in microelectronic devices. Srinivisan et al. [2] and Christensen et al. [3] identify optimal strategies in system parameters such as electrode thickness and porosity for improved performance of Lithium-ion batteries. Ramadesigan et al. [4] applied optimization to design the spatial distribution of microstructure in a porous electrode for Li-ion batteries. Many papers have been published that compute optimal temperature profiles for batch cooling seeded crystallizers (e.g., see Hu et al. [5,6] and citations therein). Although the employment of optimization based on nominal models in various applications promise improved performance with respect to the defined

objective functions, this improved performance may not be achieved in the presence of uncertainty.

Robust optimization methods have been developed to guarantee improved performance in the presence of uncertainty. These techniques have been applied to many chemical processes but have yet to be applied in the design of Lithium-ion batteries. Ma and Braatz [7] proposed an approach for the robust identification and control of batch and semibatch processes with an application to industrial crystallization. Nagy and Braatz [8] applied robust optimal techniques to the nonlinear model predictive control of batch processes using batch crystallization as a case study. Nagy and Braatz [9,10] explored the incorporation of robust performance analysis into open-loop and closed-loop optimal control design including techniques that make robust optimization techniques more tractable. Darlington et al. [11,12] report a similar framework to approximate the effects of uncertainty within the mean-variance optimization model for nonlinear systems using a batch reactor with nonlinear kinetics as a case study.

Polynomial chaos expansions have been used to perform uncertainty analysis and in robust optimization. Nagy and Braatz [13] report the use of power series and polynomial chaos expansions in distributional uncertainty analysis with application to a batch crystallization. Isukapalli et al. [14] applied PCEs to analyze uncertainty propagation in biological and environmental systems. Pan et al. [15] employed PCEs in the uncertainty analysis of direct radiative forcing by anthropogenic sulfate aerosols. Isukapalli et al. [14] employed PCE as a regression with improved sampling whereas Pan et al. [15] used a PCE variant known as probabilistic collocation. Nagy and Braatz [13] used the probabilistic collocation method in incorporating PCEs into robust optimal

design. In this work on Lithium-ion batteries, the PCE method in Isukapalli et al. [14] is applied.

In general, incorporating distributional uncertainty analysis and polynomial chaos expansions within robust optimization reduces the computationally expense significantly. While different uncertainty analysis methods have different tradeoffs in terms of accuracy and computational cost, there are significant computational savings irrespective of the method when compared to applying the classical Monte Carlo method.

CHAPTER 3: ROBUST OPTIMIZATION TECHNIQUES

3.1. Distributional robustness analysis via power series expansions

This section summarizes distributional robustness analysis using power series expansions. Define the perturbations in the model parameters and performance objective as

$$\delta\theta = \theta - \hat{\theta}, \tag{3.1}$$

$$\delta\psi = \psi - \hat{\psi}, \tag{3.2}$$

where $\theta \in R^{n_\theta}$ is the vector of perturbed model parameters, $\hat{\theta} \in R^{n_\theta}$ is the vector of nominal model parameters, ψ is a state or performance metric for the perturbed model parameter vector, and $\hat{\psi}$ is the state or performance metric for the nominal model parameter vector. One method for worst-case robustness analysis is to write $\delta\psi$ as a power series in $\delta\theta$ and employ analytical expressions or structured singular value methods to compute worst-case values for $\delta\psi$ and $\delta\theta$. Alternatively, if ψ is sufficiently differentiable with respect to the model parameter vector then ψ can be written as a Taylor's series expansion about $\hat{\theta}$ which can be used to obtain $\delta\psi$ in terms of $\delta\theta$. In both cases, accurate analyses for batch and semibatch processes have been obtained with only a few terms in the expansion (typically one or two) because for robustness analysis purposes the power series expansion only needs to be accurate for trajectories about the nominal trajectory. To illustrate the method, consider that the first-order approximation for the perturbation in performance is

$$\delta\psi = L\delta\theta, \tag{3.3}$$

$$L_i = \left.\frac{\partial\psi}{\partial\theta_i}\right|_{\theta=\hat{\theta}} \quad \forall i = 1,\ldots,n_\theta, \tag{3.4}$$

where L is the vector of sensitivities. The sensitivities may be computed analytically or numerically depending on the model equations. For example, a second-order central difference approximation for the sensitivities may be computed from

$$L_i \approx \frac{\psi(\theta_i + \Delta\theta_i) - \psi(\theta_i - \Delta\theta_i)}{2\Delta\theta_i} \quad \forall i = 1,\ldots,n_\theta. \tag{3.5}$$

The description for uncertainty in real model parameters produced by most model identification methods is the multivariate normal distribution, which can be equivalently written in terms of its hyperellipsoidal level sets

$$E_\theta = \left\{\theta : (\theta - \hat{\theta})^{\mathrm{T}} \mathbf{V}_\theta^{-1} (\theta - \hat{\theta}) \le \chi^2_{n_\theta}(\alpha)\right\}, \tag{3.6}$$

where $\mathbf{V}_\theta$ is a $n_\theta \times n_\theta$ positive-definite covariance matrix, α is the confidence level, and $\chi^2_{n_\theta}(\alpha)$ is the chi-squared distribution function with n_θ degrees of freedom. As there are few model identification algorithms that produce worst-case uncertainty descriptions, some researchers have defined a "worst-case" model uncertainty description by fixing α so that the confidence is extremely high that the model parameter vector $\theta \in R^{n_\theta}$ lies within the hyperellipsoid (3.6).

A probability density function (PDF) for the model parameters is needed to compute the PDF of the performance index. The multivariate normal distribution that describes the PDF of the model parameters is

$$f_{p.d.}(\theta) = \frac{1}{(2\pi)^{n_\theta/2} \det(\mathbf{V}_\theta)^{1/2}} \exp\left(-\frac{1}{2}(\theta - \hat{\theta})^{\mathrm{T}} \mathbf{V}_\theta^{-1} (\theta - \hat{\theta})\right). \tag{3.7}$$

When a first-order series expansion is used to relate $\delta\psi$ and $\delta\theta$ as in (3.3), then the estimated PDF of ψ is

$$f_{p.d.}(\psi) = \frac{1}{(2\pi V_\psi)^{1/2}} \exp\left(-\frac{(\psi - \hat{\psi})^2}{2V_\psi} \right), \tag{3.8}$$

where the variance of ψ is

$$V_\psi = L\mathbf{V}_\theta L^{\mathrm{T}} \tag{3.9}$$

if a first-order approximation is desired, or

$$V_\psi = L\mathbf{V}_\theta L^{\mathrm{T}} + \frac{1}{2}\mathrm{tr}\left[\mathbf{V}_\theta \mathbf{L}'\right]^2, \tag{3.10}$$

$$L'_{ij} = \left. \frac{\partial^2 \psi}{\partial\theta_i \partial\theta_j} \right|_{\theta=\hat{\theta}} \quad \forall i, j = 1, \ldots, n_\theta, \tag{3.11}$$

if a second-order approximation is desired, as in Darlington et al. [11,12], where L is given in (3.5), and $\mathbf{L}'$ is the derivative of the sensitivities with respect to the model parameters. Equation (3.10) assumes that variance of the normally distributed random variable is constant.

The above analysis holds for normally distributed random variables. In the case where model parameters are not normally distributed, a distribution transformation may be used to map them to standard random variables that are normally distributed. The above analysis can then be applied to the corresponding standard random variables, and inverse transformation can be used to obtain the original distribution of the model parameters.

When higher order series expansions than in (3.10) are used to relate $\delta\psi$ and $\delta\theta$, analytical expressions for the distribution cannot be obtained. In this case of a nonlinear relationship between ψ and θ, numerical methods must be used to compute the

probability distribution of the performance index. The PDF could be obtained by performing Monte Carlo simulation by sampling the parameter space given by the uncertainty description, but this would require a large number of samples to accurately describe regions of low probability, which is computationally expensive.

3.2. Robust optimal model-based design

An optimal design problem with one spatial dimension z is typically formulated as

$$\min_{u(z)\in U} \ \psi(x(z), \theta), \tag{3.12}$$

$$\text{s.t. } \dot{x}(z) = f(x(z), u(z), \theta), \ x(z_0) = x_0, \tag{3.13}$$

$$h(x(z), u(z), \theta) \le 0, \tag{3.14}$$

where $x(z) \in \mathrm{R}^{n_x}$ is the vector of states, $u(z) \in U$ is set of all allowed spatial distributions, $\theta \in P$ is the vector of model parameters in the uncertainty set, f is the vector function $f : \mathrm{R}^{n_x} \times U \times P \to \mathrm{R}^{n_x}$ that defines the ordinary differential equations of the system (the original system of partial differential equations is assumed to be converted into a set of ordinary differential equations using the method of lines), $h : \mathrm{R}^{n_x} \times U \times P \to \mathrm{R}^{c}$ is the vector of functions describing the spatially-varying algebraic constraints for the system, and c is the number of these constraints.

In nominal optimal design, the optimization problem (3.12) is solved by fixing $\theta = \hat{\theta}$, which yields $\hat{u}(z)$. A robust optimal design is achieved by incorporating the allowed variation in the model parameters into the optimization. One formulation is to use a multiobjective optimization, which avoids the drawbacks of the minmax optimizations often described in the literature. One objective is the value of

$\psi(\hat{x}(z), \hat{\theta})$, which is computed for the nominal parameter vector, and the other objective is the variance of $\psi(x(z), \theta)$, which incorporates parameter uncertainty:

$$J_1 = \psi(\hat{x}(z), \hat{\theta}), \tag{3.15}$$

$$J_2 = \mathrm{Var}(\psi(x(z), \theta)). \tag{3.16}$$

The variance can be computed using power series expansions or from the coefficients of a polynomial chaos expansion, which reduces the computational cost of obtaining the variance of the objective from Monte Carlo simulations or related methods. An *n*-order series expansion can be used to estimate the variance depending on the accuracy desired.

The optimization of a weighted sum of J_1 and J_2 is referred to as the mean-variance approach in the literature. That is, the multiobjective problem of minimizing the vector $J = \begin{bmatrix} J_1 & J_2 \end{bmatrix}$ is converted to a scalar problem by using the weighted sum of the objectives:

$$\begin{aligned} &\min_{u(z)\in U} \ \{J_1 + wJ_2\}, \\ &\text{s.t.} \quad \text{(3.13) and (3.14)}, \end{aligned} \tag{3.17}$$

where *w* is the weighting coefficient. The user-specified weighting coefficient *w* specifies the tradeoff between nominal and robust performance. Usually *w* is selected to correspond to the knee on a pareto-optimality plot of J_1 vs. J_2.

CHAPTER 4: POLYNOMIAL CHAOS EXPANSION

4.1. Uncertainty analysis using polynomial chaos expansions

The application of the classical Monte Carlo method in uncertainty analysis is computationally expensive, as a large number of parameter sets are required to construct the probability distribution functions of the performance index or model states/outputs. The computational expense stems from running (or solving) the model equations a large number of times. Each run might already be computationally expensive depending on the number, stiffness, and nonlinearity of the model equations (e.g., ordinary differential equations (ODEs), differential-algebraic equations (DAEs), partial differential equations (PDEs)). A computationally expensive simulation run coupled with a large number of parameter sets increases the expense for describing the distribution of the outputs. In the case where a robust optimal design is desired, an optimization routine is required. This also has a significant computation cost. The above considerations make uncertainty analysis and robust optimal design intractable with the classical Monte Carlo method except for rather simple models.

In polynomial chaos expansions (PCEs), the model outputs or performance index are expressed as simple algebraic expressions in terms of model parameters. This results in substantial reduction in computational expense, as evaluations of algebraic expressions are cheap. Uncertainty analysis and robust optimal design using PCEs involves evaluation of these algebraic expressions as opposed to actual model runs. This makes uncertainty analysis and robust optimal design more tractable. Also, the properties of distribution of the outputs or performance index may be obtained analytically for simple algebraic expressions as opposed to Monte Carlo simulations. When the parameter

uncertainties are described in terms of standard random normal variables (with mean of 0 and standard deviation of 1), a PCE can describe the model output or performance index ψ as an expansion of multidimensional Hermite polynomial functions of the uncertain parameters θ. For other types of random variables, either different polynomial bases (e.g., Legendre for the uniform distribution, Laguerre for the gamma distribution, etc.) or an appropriate transformation to standard random normal variables can be used. In this work, appropriate transformations to standard random normal variables have been used. Table 4.1 shows a few of such transformations. Using the Hermite bases in the PCE, the output can be expressed in terms of standard random normal variables $\{\theta_i\}$ using an expansion of order *k*:

$$\psi^{(k)} = a_0^{(k)}\Gamma_0 + \sum_{i_1=1}^{n_\theta} a_{i_1}^{(k)}\Gamma_1(\theta_{i_1}) + \sum_{i_1=1}^{n_\theta}\sum_{i_2=1}^{i_1} a_{i_1 i_2}^{(k)}\Gamma_2(\theta_{i_1},\theta_{i_2}) + \sum_{i_1=1}^{n_\theta}\sum_{i_2=1}^{i_1}\sum_{i_3=1}^{i_2} a_{i_1 i_2 i_3}^{(k)}\Gamma_3(\theta_{i_1},\theta_{i_2},\theta_{i_3}) + \cdots, \quad (4.1)$$

where n_θ is the number of parameters, the $a_0^{(k)}$, $a_{i_1}^{(k)}$, $a_{i_1 i_2}^{(k)}$, $a_{i_1 i_2 i_3}^{(k)}$,… are deterministic real coefficients to be estimated, and the multidimensional Hermite polynomials of degree $m = i_1, i_2, ..., i_{n_\theta}$ are

$$\Gamma_m(\theta_{i_1},...,\theta_m) = (-1)^m e^{\theta^T\theta/2}\frac{\partial^m e^{-\theta^T\theta/2}}{\partial\theta_1\cdots\partial\theta_m}. \quad (4.2)$$

The polynomial chaos terms are random variables since they are functions of the random variables, and terms of different order are orthogonal to each other (with respect to an inner product defined in Gaussian measures as the expected value of the product of two random variables, i.e., $E[\Gamma_i\Gamma_j] = 0$ for $\Gamma_i \neq \Gamma_j$). In addition, polynomial chaos terms of the same order but with a different argument list are also orthogonal ($E[\Gamma_m(\{\theta\}_i)\Gamma_m(\{\theta\}_j)] = 0, i \neq j$). In PCEs, any form of polynomials could be used but the properties of

orthogonal polynomials make the uncertainty analysis more efficient. As an example, the expected value of both sides of equation (4.1) results in the expected value of ψ being simply $E[\psi^{(k)}] = a_0^{(k)}\Gamma_0$. The calculation of other statistical measures is also significantly simplified by using the properties of orthogonality. Another example is in computing the variance of ψ which is given as $\sigma^2 = \sum_{i=1} a_i^2 E\{(\Gamma_i(\{\theta\}_i)^2\}$ [16]. The orthogonal polynomials are derived from the probability distribution of the parameters using the orthonormality condition:

$$\int_{\theta} f_{\text{d.f.}}(\theta)\Gamma_i(\theta)\Gamma_j(\theta) = \delta_{ij} \quad \text{where } \delta_{ij} = 1 \text{ if } i = j,\ \delta_{ij} = 0 \text{ if } i \neq j. \tag{4.3}$$

Since $\Gamma_0(\theta) = 1$, the first-order Hermite polynomial can be calculated from

$$\int_{\theta} f_{\text{d.f.}}(\theta_1)\Gamma_1(\theta_1)(1) = 0 \tag{4.4}$$

and the procedure can be repeated to obtain all terms in the PCE. Table 4.2 shows a few Hermite polynomials up to order 4. The number of coefficients in the PCE depends on the number of uncertain parameters and the order of expansion and can be calculated from $N_a = (n_\theta + k)!/\, n_\theta!k!$ (e.g., there are 6 coefficients for two parameters and a second-order PCE and 15 coefficients for a fourth-order PCE, where as for four uncertain parameters there are 15 coefficients for a second-order PCE and 70 for a fourth-order PCE); however, it is not necessary to use higher order than three or four for most engineering applications. Table 4.3 shows relationships between the number of coefficients in the PCE and the number of uncertain parameters up to a fourth-order PCE. The polynomial chaos expansion is convergent in the mean-square sense, therefore the coefficients in the PCE are calculated using least-squares minimization considering

sample input/output pairs from the model, so that the best fit is achieved between the PCE and the nonlinear model (or experimental data).

There are two main methods for sampling input/output pairs, and hence computing the coefficients of the PCE: (i) the probabilistic collocation method (PCM), and (ii) the regression method with improved sampling (RMIS). Both methods are weighted-residual schemes, which differ in the way sampling points are chosen. PCM uses the principle of collocation, which imposes that ψ is exact at a set of chosen collocation points, thus making the residual between the output of PCE and the output of the complex nonlinear model (or experiment) at those points equal to zero. RMIS is primarily an extension of PCM. In PCM, the number of collocation points is set to equal the number of unknown coefficients, which are found by solving a set of linear equations generated from the outputs from the original model (or experiment). In RMIS, more collocation points than in PCM are chosen, and hence there are more equations than unknown coefficients, which are found by solving an overdetermined system of linear equations. The additional number of points selected increases the accuracy in determining the coefficients. Another difference between both methods is how the collocation points are selected. In most cases the number of available collocation points exceeds the number of coefficients to be determined. In both cases the collocation points are chosen from the roots of the orthogonal polynomial of a degree one higher than the order of the PCE. In PCM, the collocation points are chosen randomly since we usually have more collocation points than coefficients. In RMIS, the collocation points are chosen systematically such that the collocation points selected correspond to regions of higher probability (for example, if standard random normal variables are used, collocation points closer to 0 are

selected in preference to those further, and a second criteria might be symmetry of the points selected). The collocation points selected affects the accuracy of the approximation, which makes the RMIS superior to PCM. In this work the regression method with improved sampling is used to calculate the coefficients. Further accuracy in estimating coefficients may be achieved by using information about the sensitivities at the collocation points.

When a dynamic simulation algorithm is used, numerical errors will occur in the sampled input/output pairs, and when experimental data are used, the measurements usually have noise and are affected by unmeasured disturbances. For both cases, it may be less attractive to use a collocation method in the construction of the PCE. The effect of numerical errors, measurement noise, and unmeasured disturbances can be reduced using extra input/output pairs and/or employing regularization methods with least squares.

PCE utilizes a simpler representation of the simulation model, and this representation can be used to compute the pdf of the outputs (via Monte Carlo method or via the contour mapping approach). Also, the PCE can be used to analytically compute statistical measures, such as the mean, variance, or higher order moments of the outputs because of the principle orthogonality. This allows for construction of pdf of the outputs from the moments of the distribution without applying the Monte Carlo method or the contour mapping approach.

4.2. Example

Consider a model with three independent random variables inputs X_1, X_2, and X_3, and three outputs Y_1, Y_2, and Y_3, where the distribution of the input random variables are given by

$$\begin{aligned} X_1 &= \text{Uniform}(p_1, q_1) \\ X_2 &= \text{Normal}(p_2, q_2) \\ X_3 &= \text{Lognormal}(p_3, q_3). \end{aligned} \tag{4.5}$$

The input random variables can be represented by three standard normal random variables θ_1, θ_2, and θ_3 using Table 4.1 as

$$\begin{aligned} X_1 &= p_1 + (q_1 - p_1)\left(\frac{1}{2} + \frac{1}{2}\text{erf}(\theta_1/\sqrt{2})\right) \\ X_2 &= p_2 + q_2\theta_2 \\ X_3 &= \exp(p_3 + q_3\theta_3), \end{aligned} \tag{4.6}$$

where θ_1, θ_2, and θ_3 are distributed with mean 0 and standard deviation 1. A second-order polynomial chaos expansion for Y_1, Y_2, and Y_3 in terms of θ_1, θ_2, and θ_3 is given by

$$\begin{aligned} Y_1 &= a_0 + a_1\theta_1 + a_2\theta_2 + a_3\theta_3 + a_4(\theta_1^2 - 1) + a_5(\theta_2^2 - 1) + a_6(\theta_3^2 - 1) + a_7\theta_1\theta_2 + a_8\theta_2\theta_3 + a_9\theta_1\theta_3 \\ Y_2 &= b_0 + b_1\theta_1 + b_2\theta_2 + b_3\theta_3 + b_4(\theta_1^2 - 1) + b_5(\theta_2^2 - 1) + b_6(\theta_3^2 - 1) + b_7\theta_1\theta_2 + b_8\theta_2\theta_3 + b_9\theta_1\theta_3 \\ Y_3 &= c_0 + c_1\theta_1 + c_2\theta_2 + c_3\theta_3 + c_4(\theta_1^2 - 1) + c_5(\theta_2^2 - 1) + c_6(\theta_3^2 - 1) + c_7\theta_1\theta_2 + c_8\theta_2\theta_3 + c_9\theta_1\theta_3 \end{aligned} \tag{4.7}$$

The number of coefficients in each expansion can be calculated *a priori* by using the equations in Table 4.3. In order to estimate the 10 coefficients (for each output) of the expansions above, at least 10 sets of sample points must be chosen. The number of sets *N* chosen is as recommended in the efficient collocation method (ECM) or RMIS, which equals about twice the number of coefficients, i.e., 20 in this case. The sets have the form given by

$$(\theta_{1,1}, \theta_{2,1}, \theta_{3,1}), (\theta_{1,2}, \theta_{2,2}, \theta_{3,2}), \cdots, (\theta_{1,N}, \theta_{2,N}, \theta_{3,N}). \tag{4.8}$$

The sample points are generated from the roots of the Hermite polynomial of *order* + 1, where *order* is the order of the expansion. In this example, the roots of the Hermite polynomial of order 3 are used. The selection of the sample points is as discussed in Isukapalli et al. [14].

These sample points corresponding to the original model input samples

$$(x_{1,1}, x_{2,1}, x_{3,1}), (x_{1,2}, x_{2,2}, x_{3,2}), \cdots, (x_{1,N}, x_{2,N}, x_{3,N}), \tag{4.9}$$

are

$$\begin{pmatrix} \theta_{1,i} \\ \theta_{2,i} \\ \theta_{3,i} \end{pmatrix} \rightarrow \begin{pmatrix} x_{1,i} \\ x_{2,i} \\ x_{3,i} \end{pmatrix} = \begin{pmatrix} p_1 + (q_1 - p_1)\left(\frac{1}{2} + \frac{1}{2}\mathrm{erf}(\theta_{1,i}/\sqrt{2})\right) \\ p_2 + q_2\theta_{2,i} \\ \exp(p_3 + q_3\theta_{3,i}) \end{pmatrix}, \ \forall i = 1, \cdots, N \tag{4.10}$$

After obtaining the original model input sample points, the model simulation or experiment is performed at the points given by $(x_{1,1}, x_{2,1}, x_{3,1}), \cdots, (x_{1,N}, x_{2,N}, x_{3,N})$. Then the outputs at these sample points $y_{1,1}, \cdots, y_{1,N}, y_{2,1}, \cdots, y_{2,N}$, and $y_{3,1}, \cdots, y_{3,N}$, are used to compute the coefficients $a_0, \cdots, a_9, b_0, \cdots, b_9$, and $c_0, \cdots, c_9$, by solving the following linear equations using the singular value decomposition:

$$Z^{\mathrm{T}} \begin{bmatrix} a_0 & b_0 & c_0 \\ a_1 & b_1 & c_1 \\ \vdots & \vdots & \vdots \\ a_8 & b_8 & c_8 \\ a_9 & b_9 & c_9 \end{bmatrix} = \begin{bmatrix} y_{1,1} & y_{2,1} & y_{3,1} \\ y_{1,2} & y_{2,2} & y_{3,2} \\ \vdots & \vdots & \vdots \\ y_{1,N} & y_{2,N} & y_{3,N} \end{bmatrix}, \tag{4.11}$$

where

$$Z = \begin{bmatrix} 1 & 1 & 1 & \cdots & 1 \\ \theta_{1,1} & \theta_{1,2} & \theta_{1,3} & \cdots & \theta_{1,N} \\ \theta_{2,1} & \theta_{2,2} & \theta_{2,3} & \cdots & \theta_{2,N} \\ \theta_{3,1} & \theta_{3,2} & \theta_{3,3} & \cdots & \theta_{3,N} \\ \theta_{1,1}^2 - 1 & \theta_{1,2}^2 - 1 & \theta_{1,3}^2 - 1 & \cdots & \theta_{1,N}^2 - 1 \\ \theta_{2,1}^2 - 1 & \theta_{2,2}^2 - 1 & \theta_{2,3}^2 - 1 & \cdots & \theta_{2,N}^2 - 1 \\ \theta_{3,1}^2 - 1 & \theta_{3,2}^2 - 1 & \theta_{3,3}^2 - 1 & \cdots & \theta_{3,N}^2 - 1 \\ \theta_{1,1}\theta_{2,1} & \theta_{1,2}\theta_{2,2} & \theta_{1,3}\theta_{2,3} & \cdots & \theta_{1,N}\theta_{2,N} \\ \theta_{2,1}\theta_{3,1} & \theta_{2,2}\theta_{3,2} & \theta_{2,3}\theta_{3,3} & \cdots & \theta_{2,N}\theta_{3,N} \\ \theta_{1,1}\theta_{3,1} & \theta_{1,2}\theta_{3,2} & \theta_{1,3}\theta_{3,3} & \cdots & \theta_{1,N}\theta_{3,N} \end{bmatrix}. \tag{4.12}$$

In the above equations, the only unknowns are $a_0, \cdots, a_9$, $b_0, \cdots, b_9$, and $c_0, \cdots, c_9$, since Z can be calculated from the sample points selected. Once the coefficients are estimated, the distributions of Y_1, Y_2, and Y_3 are fully described by the polynomial chaos expansions as shown in (4.7). The value of X can be computed from

$$X = (ZZ^T)^{-1} ZY \tag{4.13}$$

In obtaining the statistical properties of the outputs from the polynomial chaos expansions, there are three possible routes. First, some of the statistical properties may be obtained analytically, for example, the mean as discussed above. Second, a large number of random samples $(\theta_{1,i}, \theta_{2,i}, \theta_{3,i})$ could be numerically generated, and then the corresponding values of model inputs and outputs are calculated. Alternatively, a large number of model input samples $(x_{1,i}, x_{2,i}, x_{3,i})$ could be numerically generated, and then the corresponding standard random variables (from equations in Table 4.1) and model outputs are calculated. The statistical properties can then be computed from the values of inputs and outputs.

Table 4.1. Transformations between standard normal random variable and common univariate distributions.

Distribution type	Transformation from standard random normal variable to distribution type[m]	Transformation from distribution type to standard random normal variable[n]
Uniform (a, b)	$a+(b-a)\left(\frac{1}{2}+\frac{1}{2}\text{erf}(\theta/\sqrt{2})\right)$	$\sqrt{2}\text{erf}^{-1}\left(\frac{2X-(b+a)}{b-a}\right)$
Normal(μ,σ)	$\mu+\sigma\theta$	$\frac{X-\mu}{\sigma}$
Lognormal(μ,σ)	$\exp(\mu+\sigma\theta)$	$\frac{\log X-\mu}{\sigma}$
Gamma (a, b)	$ab\left(\theta\sqrt{\frac{1}{9a}}+1-\frac{1}{9a}\right)^3$	$\sqrt{9a}\left(\left(\frac{X}{ab}\right)^{\frac{1}{3}}+\frac{1}{9a}-1\right)$
Exponential(λ)	$-\frac{1}{\lambda}\log\left(\frac{1}{2}+\frac{1}{2}\text{erf}(\theta/\sqrt{2})\right)$	$\sqrt{2}\text{erf}^{-1}\left(2\exp(-\lambda X)-1\right)$
Weibull(a)	$y^{\frac{1}{a}}$	X^a
Extreme Value	$-\log(y)$	$\exp(-X)$

[m] θ is normal (0,1) and y is exponential (1) distributed

[n] X is sampled from distribution type

Table 4.2. Hermite polynomials of order up to 4.

Order	Hermite polynomial
0	1
1	$\theta/\sqrt{1!\sqrt{2\pi}}$
2	$\theta^2-1/(\sqrt{2!\sqrt{2\pi}})$
3	$\theta^3-3\theta/(\sqrt{3!\sqrt{2\pi}})$
4	$\theta^4-6\theta^2+3/(\sqrt{4!\sqrt{2\pi}})$

Table 4.3. Number of coefficients in a PCE as a function of number of uncertain parameters n_θ and the order of the expansion.

Order of PCE	Number of coefficients
1	$1+n_\theta$
2	$1+2n_\theta+\frac{n_\theta(n_\theta-1)}{2}$
3	$1+3n_\theta+\frac{3n_\theta(n_\theta-1)}{2}+\frac{n_\theta(n_\theta-1)(n_\theta-2)}{6}$
4	$1+4n_\theta+\frac{4n_\theta(n_\theta-1)}{2}+\frac{4n_\theta(n_\theta-1)(n_\theta-2)}{6}+\frac{n_\theta(n_\theta-1)(n_\theta-2)(n_\theta-3)}{12}$

CHAPTER 5: ROBUST OPTIMIZATION AND LI-ION BATTERIES

5.1. Robust optimal design of Li-ion batteries

Robust optimization techniques are applied in the design of Li-ion batteries with different degrees of spatially-varying porosity. The mathematical model [4] is

$$x^{\mathrm{T}} = [i_1, \varphi_1, \varphi_2],$$
$$f(x,u,\theta) = \begin{bmatrix} -ai_0 \dfrac{F}{RT}(\varphi_1 - \varphi_2) l_p \\ -\dfrac{i_1 l_p}{\sigma} \\ \dfrac{(i_1 - i_{app}) l_p}{\kappa} \end{bmatrix}, \tag{5.1}$$

where i_1 is the solid-phase current, φ_1 is the solid-phase potential, φ_2 is the electrolyte-phase potential, a is the active surface area given by

$$a = \frac{3(1-\varepsilon(z))}{R_p}, \tag{5.2}$$

T is the temperature, R is the gas constant, F is the Faraday constant, l_p is the length of the positive porous electrode, i_0 is the applied current density, R_p is the particle radius of active materials, i_{app} is the exchange current density

$$i_{app} = -\sigma(z) \left. \frac{d\varphi_1}{dz} \right|_{z=0} \tag{5.3}$$

$\varepsilon(z)$ is the porosity, which varies as a function of distance, z, $\sigma(z)$ and $\kappa(z)$ are the electronic and ionic conductivities respectively, which vary as function of distance as

$$\sigma(z) = \sigma_0 (1-\varepsilon(z)), \tag{5.4}$$

$$\kappa(z) = \kappa_0 \varepsilon(z)^{brugg}, \tag{5.5}$$

because of their porosity dependence, where *brugg* is the Bruggman coefficient which accounts for the tortuous path in the porous electrode. The model parameter vector consists of the voltage, and the material properties of the solid and electrolyte-phase

$$\theta^{\mathrm{T}} = \begin{bmatrix} V & \sigma_0 & \kappa_0 & i_0 & R_p \end{bmatrix}, \tag{5.6}$$

with nominal values:

$$\hat{\theta}_1^{\mathrm{T}} = \begin{bmatrix} 1 & 100 & 20 & 0.01 & 5e-6 \end{bmatrix}, \tag{5.7}$$

and the uncertainty descriptions characterized by the covariance matrix

$$V_{\theta,1}^{-1} = \begin{bmatrix} 0.0101 & -0.0238 & 0.0042 & 3.11e-08 & 3.04e-10 \\ -0.0238 & 102.40 & 0.1456 & -2.05e-05 & 4.94e-08 \\ 0.0042 & 0.1456 & 4.2466 & -2.28e-06 & 2.95e-08 \\ 3.11e-08 & -2.05e-05 & -2.28e-06 & 9.42e-09 & 8.35e-13 \\ 3.04e-10 & 4.94e-08 & 2.95e-08 & 8.35e-13 & 2.55e-13 \end{bmatrix}. \tag{5.8}$$

The optimization variable is the porosity distribution, which has dimensions depending on the degree of spatial variation:

$$u(z) = \varepsilon(z). \tag{5.9}$$

Although there are discontinuities in the porosity distribution, the model is defined such that the current and potentials are continuously differentiable.

The optimization objective considered is the minimization of the ohmic resistance across the electrode:

$$\psi = \frac{V}{i_{app}}. \tag{5.10}$$

In the robust case, the optimization objective includes the minimization of the ohmic resistance and its variance. The effect of uncertainties in the model parameters on the ohmic resistance at a base uniform porosity ($\varepsilon = 0.4$) and nominally optimized uniform

porosity (ε = 0.21388) are compared in Fig. 5.1, which were computed using the Monte Carlo method, which is implementable for this simple example.

The sensitivities computed for the first-order approximation of the variance are

$$L_1 = \begin{bmatrix} 0.0111 & -9.75e-05 & 4.87e-04 & 0 & 2.61e-12 \end{bmatrix}, \tag{5.11}$$

The optimization problem (5.1)-(5.3) was solved with the constraints:

$$h(x,u,\theta) = \begin{bmatrix} \varepsilon_j - \varepsilon_{\max} \\ -\varepsilon_j + \varepsilon_{\min} \end{bmatrix} \leq 0\,, \tag{5.12}$$

where $\varepsilon_{\min}$ and $\varepsilon_{\max}$ are the minimum and maximum porosity *practically* attainable. The optimization problem was solved using the sequential simulation-optimization approach.

Sequential Simulation-Optimization Approach

Step 1: ψ was optimized over the model parameters and the optimal ψ and the corresponding Var(ψ) were computed.

Step 2: on a plot of ψ vs. Var(ψ) for the optimized model parameters in Step 1, a point was placed on the plot (this point corresponds to $w = 0$). Collectively, Steps 1 and 2 compute the nominal optimal porosity profile.

Step 3: w was set based on ψ/Var(ψ) from Step 2.

Step 4: $\psi + w$Var(ψ) was optimized over the model parameters and the corresponding ψ and Var(ψ) were reported.

Step 5: on a plot of ψ vs. Var(ψ) for the optimized model parameters in Step 4, another point was placed on the plot (this point corresponds to a nonzero w).

Step 6: w was set to a value between 0 and the value in Step 3 to fill in points on the pareto-optimality curve between the points produced by Steps 2 and 5, or w was

set to a larger value to extend the pareto-optimality curve beyond the points in Steps 2 and 5

Step 7: Step 4 was repeated for the new *w*.

Step 8: step 5 was repeated for the next *w*.

Step 9: Steps 6-8 were repeated until the pareto-optimality curve was mapped out with a reasonably uniform spacing points on the curve

The robust optimal porosity profile was specified by the knee of the pareto-optimality curve obtained from Steps 1-9. This knee corresponds to the point where no large improvements in ψ or Var(ψ) are obtainable by changing the value for *w*.

5.2. Results and discussion

The nominal and robust optimal porosity profiles are shown in Figs. 5.2 and 5.3. The robust optimal profile is obtained from the pareto-optimality curves in Fig. 5.4. From Figs. 5.2 and 5.3, it can be observed that the nominal and robust porosity profiles differ considerably at the beginning of the electrode and converge towards the end of the electrode, which is consistent with the results from performing Monte Carlo simulations on the model. The simulation results show that the effect of uncertainty in the parameters diminishes as we move down the electrode. This is expected as the boundary conditions in the model require that some conditions be satisfied at the end of the electrode. The probability distribution functions for the current, solid-phase potential, and electrolyte-phase potential are shown in Fig. 5.5. It can be observed from Fig. 5.5 that the uncertainties in the current and electrolyte-phase potential reduce while that in the solid-phase potential remains the same as we move down the electrode. The pareto-optimality curves show that there are advantages of exploring profiles with increasing degrees of

porosity. The ohmic resistance and its variance reduce as the degree of porosity increases. Although a linear profile might appear intuitive, the results from both the nominal and robust optimization show that the optimal porosity profiles do not follow a simple non-decreasing or non-increasing description. Even if the descriptions are simple, the fabrication of batteries with high degrees of porosity variation is debatable.

It should also be noted from Fig. 5.1 that the variance in the ohmic resistance for the base porosity is smaller than for the nominally optimal porosity. This may explain the reason why there are no significant improvements when Pareto-optimality is explored. Since the model for the Li-ion battery considered only one electrode, a full Li-ion battery model may be necessary to observe significant improvements when robust optimization techniques are applied.

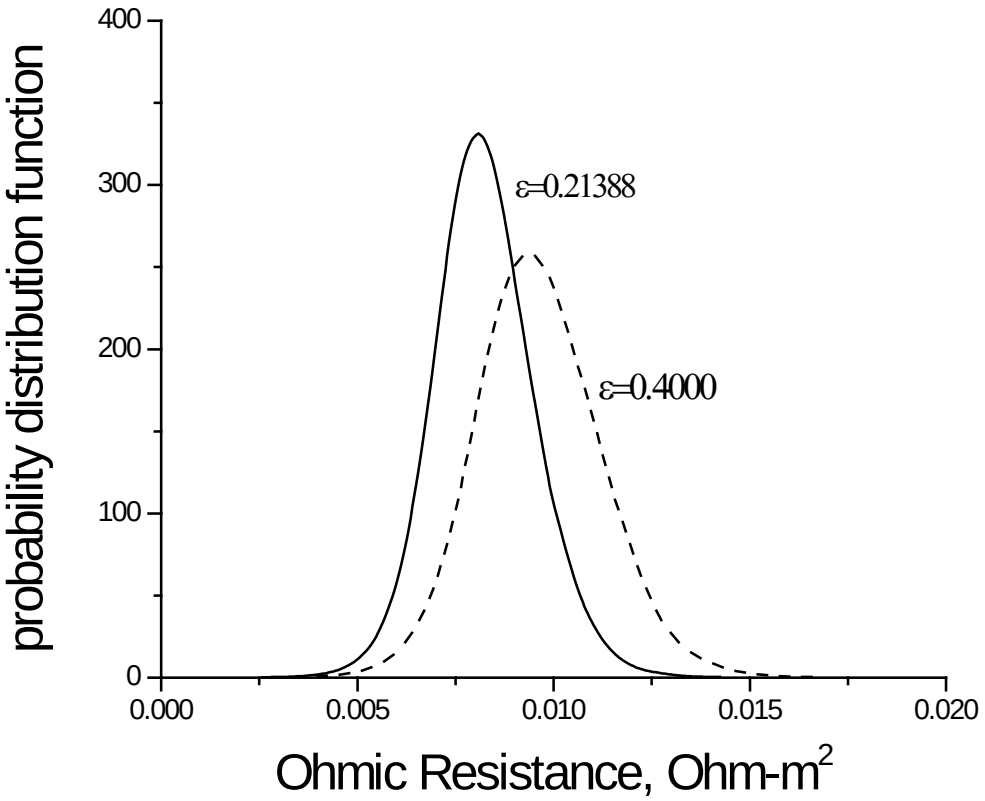

Fig. 5.1. Probability distribution function for the ohmic resistance for electrodes with spatially-uniform porosities of $\varepsilon = 0.4$ (base) and obtained by optimization ($\varepsilon = 0.21388$).

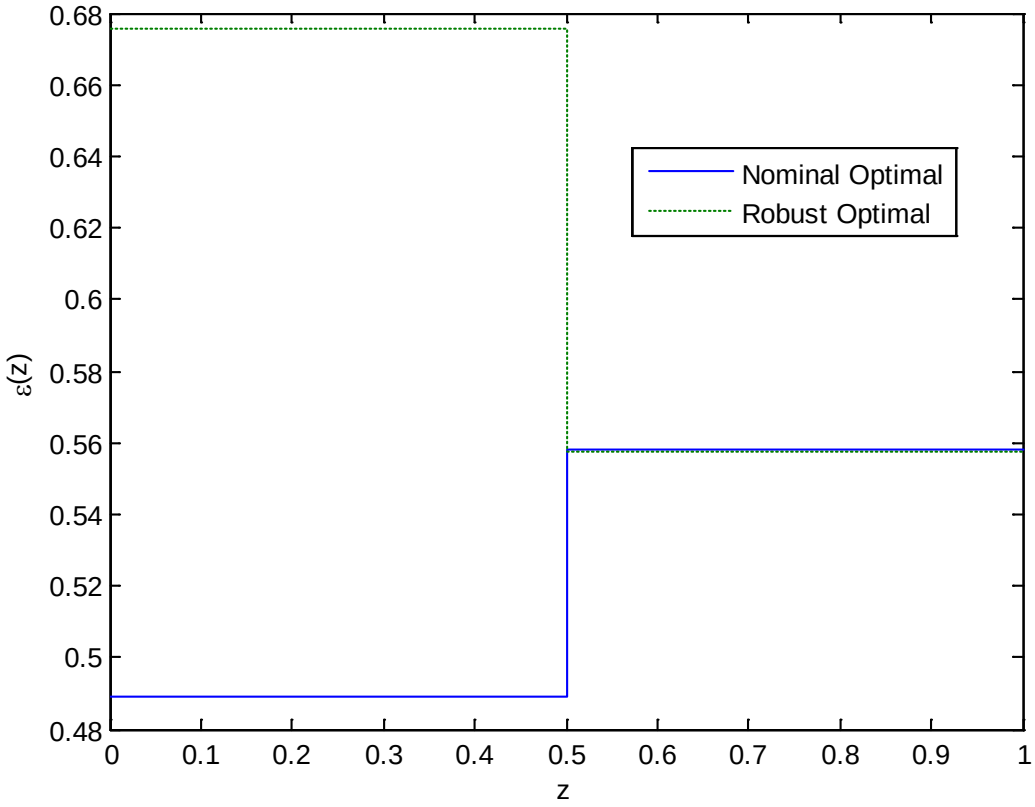

Fig. 5.2. Nominal optimal porosity profile and the robust optimal profile with porosity allowed to have a different value on each half of the electrode.

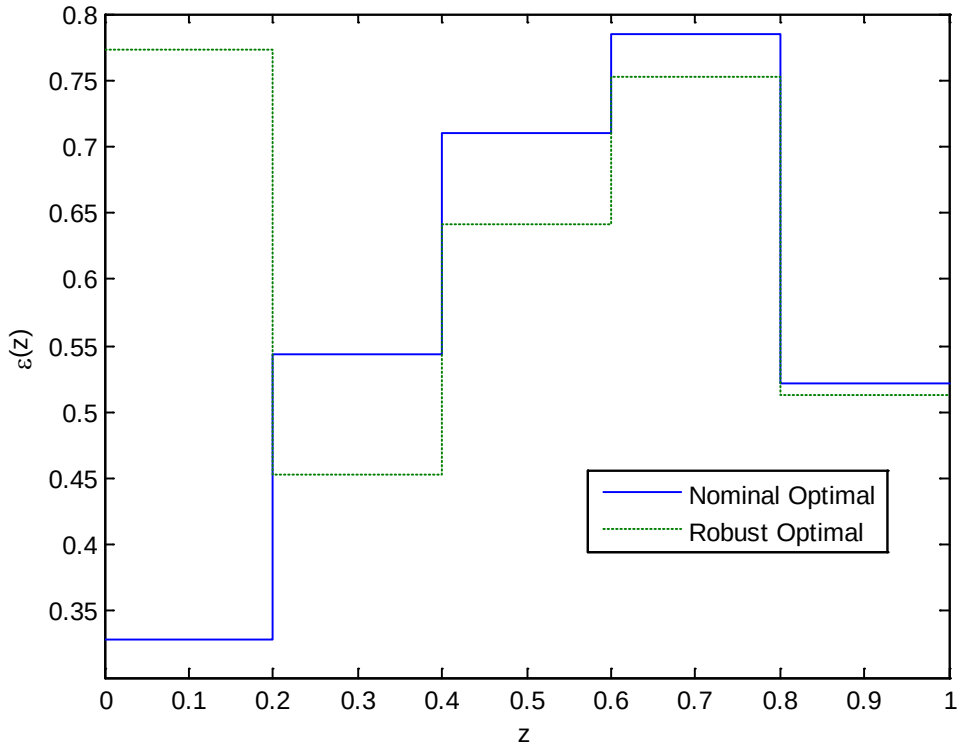

Fig. 5.3. Nominal optimal porosity profiles and robust optimal profile with five different values allowed for equal portions of the electrode.

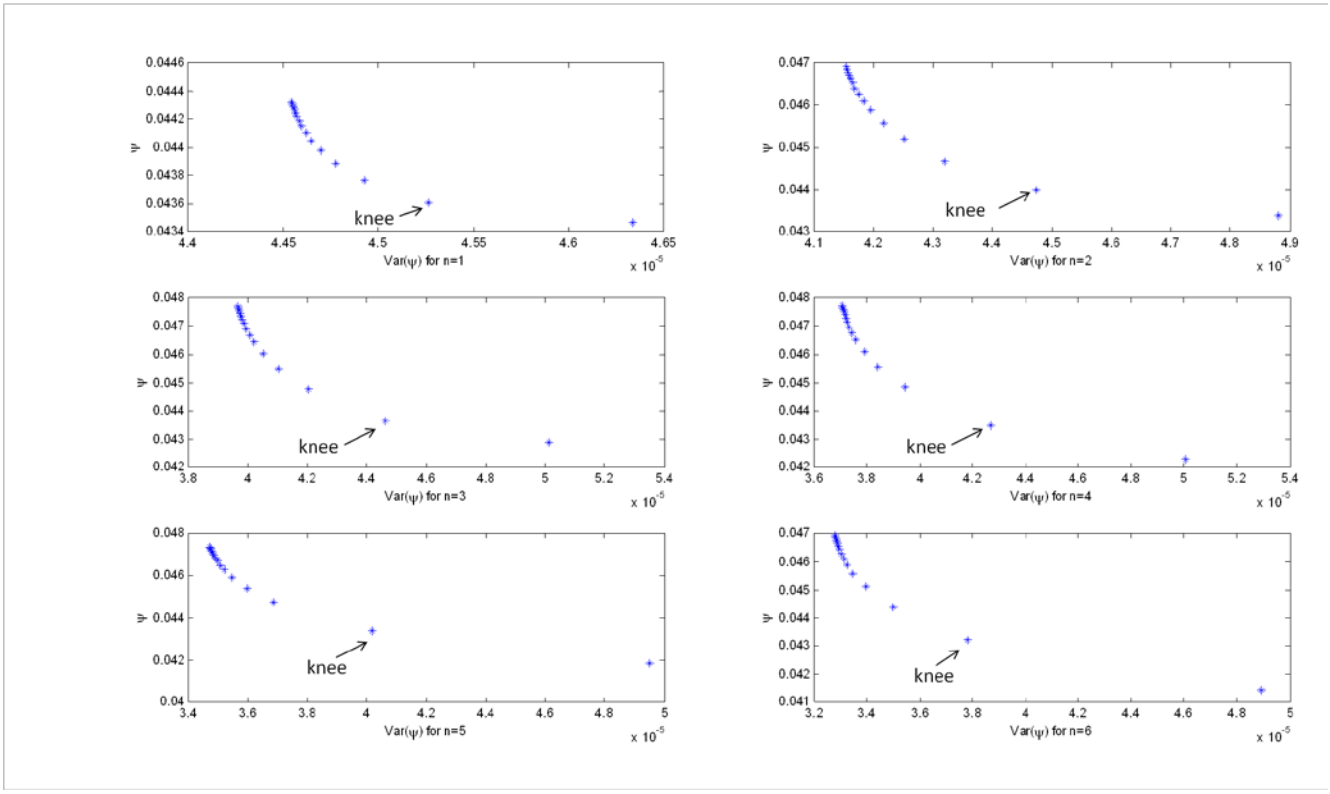

Fig. 5.4. Pareto-optimality curve for varying degrees of porosities, with the knee corresponding to the robust optimal porosity profile.

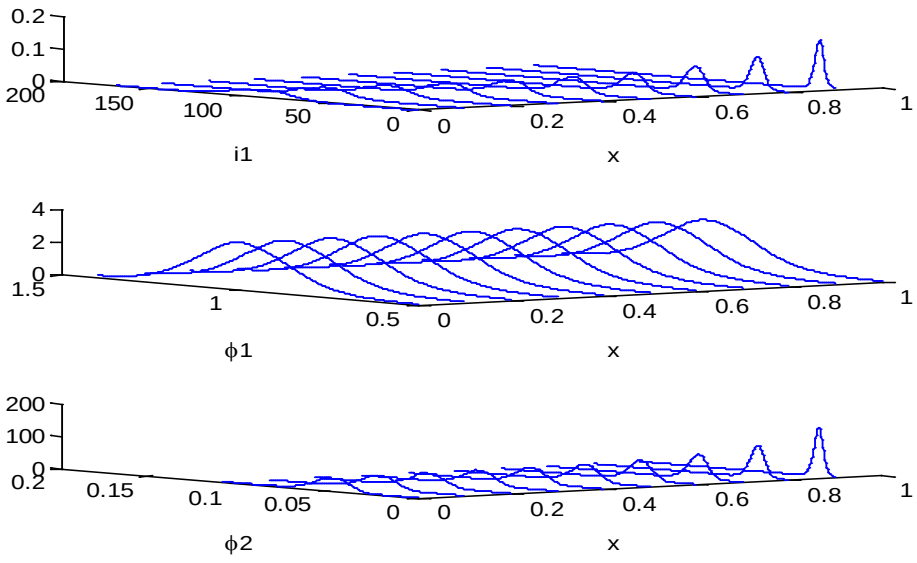

Fig. 5.5. Variation of the PDF of the current, solid-phase potential, and electrolyte-phase with distance *x* across the electrode.

CHAPTER 6: PCE-BASED APPROACH TO ROBUST OPTIMIZATION

As discussed in Chapter 3, the robust optimization problem is usually posed as a multiobjective optimization (3.17). It is necessary to compute the variance of the objective function with respect to parametric uncertainties in performing robust optimization. The variance may be computed by methods discussed in Chapter 3 or analytically from the coefficients of a polynomial chaos expansion when the objective function is expressed as a function of Hermite polynomials of the uncertain parameters. The main idea in this approach is to consider the design or control variables as uncertain parameters (within a reasonable range), and express the objective function as function of the Hermite polynomials in the uncertain parameters and the design variables. This new functional form allows for quick computation of the variance of the objective function and also a polynomial expression for the multiobjective optimization problem, which simplifies the determination of the robust optimal values for the design variables. Mathematically, this idea may be expressed as

$$y = f(x,u,\theta) = g(x,\theta_{new}(u,\theta)). \tag{6.1}$$

The methods for PCE discussed in Chapter 4 can then be applied to g. Two cases are used to illustrate this new approach: a well-studied crystallization problem and the Li-ion battery problem.

6.1 Application to simulated batch crystallization problem

The crystallization problem uses the mathematical formulation in the study by Nagy and Braatz [13]. The optimal control problem is posed as

$$\underset{T(k)}{\text{optimize}}\ J \tag{6.2}$$

subject to the ODE with

$$f(x,u,\theta)=\begin{bmatrix} B \\ G\mu_0 \\ 2G\mu_1 \\ 3G\mu_2 \\ 4G\mu_3 \\ -\rho_c k_v 3G\mu_2 \\ G\mu_{seed,0} \\ 2G\mu_{seed,1} \\ 3G\mu_{seed,2} \end{bmatrix} \tag{6.3}$$

and constraints

$$\begin{aligned} & T_{\min}(k) \le T(k) \le T_{\max}(k) \\ & R_{\min}(k) \le \frac{dT(k)}{dt} \le R_{\max}(k) \\ & C_{final} \le C_{final,\max} \end{aligned} \tag{6.4}$$

where the objective function J is a function of the states, $x^{\mathrm{T}} = \begin{bmatrix} \mu_0 & \mu_1 & \mu_2 & \mu_3 & \mu_4 & \mu_{seed,0} & \mu_{seed,1} & \mu_{seed,2} & \mu_{seed,3} \end{bmatrix}$, and is a representative property of the final crystal size distribution. For example, we may consider the nucleation-mass-to-seed mass ratio ($J_{n.s.r.}$), coefficient of variation ($J_{c.v.}$) and weight-mean size of the crystals ($J_{w.m.s.}$):

$$J_{n.s.r.} = (\mu_3 - \mu_{seed,3})/\mu_{seed,3} \tag{6.5}$$

$$J_{c.v..} = (\mu_2\mu_0/(\mu_1)^2 - 1)^{1/2} \tag{6.6}$$

$$J_{w.m.s.} = \mu_4/\mu_3 \tag{6.7}$$

The equality constraints (6.3) are the model equations, with initial conditions given by Chung et al., where μ_i is the ith moment (i = 0,…,4) of the total crystal phase, $\mu_{seed,j}$ is the jth moment (j = 0,...,3) corresponding to the crystals grown from seed, C is the solute

concentration, T is the temperature, r_0 is the size of crystal nuclei, k_v is the volumetric shape factor, and ρ_c is the density of the crystal. The rate of crystal growth is given by

$$G = k_g S^g, \tag{6.8}$$

$$B = k_b S^b \mu_3, \tag{6.9}$$

where $S = (C_{sat} - C)/C_{sat}$ is the relative supersaturation, and $C_{sat} = C_{sat}(T)$ is the saturated concentration. The model parameter vector consists of growth and nucleation kinetic parameters

$$\theta^{\mathrm{T}} = \begin{bmatrix} g & k_g & b & k_b \end{bmatrix} \tag{6.10}$$

with nominal values

$$\hat{\theta}^{\mathrm{T}} = \begin{bmatrix} 1.31 & \exp(8.79) & 1.84 & \exp(17.38) \end{bmatrix} \tag{6.11}$$

with the uncertainty description in the form (3.6) characterized by the covariance matrix

$$V_\theta^{-1} = \begin{bmatrix} 102873 & -21960 & -7509 & 1445 \\ -21960 & 4714 & 1809 & -354 \\ -7509 & 1809 & 24225 & -5198 \\ 1445 & -354 & -5198 & 1116 \end{bmatrix}. \tag{6.12}$$

$T_{\min}$, $T_{\max}$, $R_{\min}$, and $R_{\max}$ in (6.4) are the minimum and maximum temperatures and temperature ramp rates, respectively. The first two inequalities ensure that the crystallizer operates within a certain profile. The last constraint ensures the solute concentration at the end of the batch is less than some maximum value set by economic constraint.

The above optimization was solved by Nagy and Braatz [13] to compare uncertainty analysis schemes for an optimal control problem. The objective function was the nucleation to seed mass ratio ($J_{n.s.r.}$). This thesis uses a variant of the optimal

temperature profile obtained by Nagy and Braatz (see Fig. 6.1). In demonstrating our approach, the transformed vector of parameters is

$$\theta_{new}^{\mathrm{T}} = \begin{bmatrix} g & k_g & b & k_b & T_0 & T_{40} & T_{80} & T_{120} & T_{160} \end{bmatrix}, \tag{6.13}$$

with nominal values

$$\hat{\theta}_{new}^{\mathrm{T}} = \begin{bmatrix} 1.31 & \exp(8.79) & 1.84 & \exp(17.38) & 32 & 31.65 & 31.49 & 30.95 & 28 \end{bmatrix}. \tag{6.14}$$

The uncertainty description for the kinetic parameters remains the same, while that for the temperatures are described by equal standard deviations of 0.01°C, 0.1°C, and 1°C for different studies.

In determining the PCE, at least a second-order expansion is required to compute the variance from the coefficients. For a second-order expansion with 9 parameters, 55 coefficients need to be determined, with 54 of them contributing to the estimate of the variance. The coefficients were determined using the probabilistic collocation method with the constraint that the first coefficient equals the mean of the distribution. It should be noted that the parameters are first transformed appropriately to standard random variables before the coefficients are determined. Table 6.1 shows that the accuracy in the estimates of the variance is ~10%, which is accurate enough for use in robust design or control. In terms of computational cost, the computation of the variance from the PCE coefficients was essentially instantaneous, while the computation of the variance by applying the Monte Carlo method to the PCE took about 16 s.

6.2. Application to the design of spatially-varying Li-ion batteries

The model equations used in this section are the same as those used in Chapter 5. A spatially-varying electrode with two possible values for the porosity in an electrode is studied. The new parameter vector is given by

$$\theta_{new}^{\mathrm{T}} = \begin{bmatrix} V & \sigma_0 & \kappa_0 & i_0 & R_p & \varepsilon_1 & \varepsilon_2 \end{bmatrix}, \tag{6.15}$$

with nominal parameters

$$\hat{\theta}_{new}^{\mathrm{T}} = \begin{bmatrix} 1 & 100 & 20 & 0.01 & 5e-6 & 0.55 & 0.50 \end{bmatrix}, \tag{6.16}$$

where ε_1 and ε_2 are the porosities in regions 1 and 2, respectively. The uncertainties in the first five parameters were described by normal distributions with standard deviations that are 10% of their nominal values, while the porosities were described by a uniform distribution with an upper bound of 0.60.

The PCE in the new parameter set was obtained for the objective function (the ohmic resistance, as defined in Chapter 5). An expansion of order 2 requires the determination of 36 coefficients, and an expansion of order 3 requires the determination of 120 coefficients. The probabilistic collocation method was used to determine the coefficients without any restrictions. The parameters were first transformed to standard normal variables so that the coefficients are related directly to the mean and the variance of the resulting distribution. Table 6.2 shows the results for various schemes for computing the variance. Within three significant figures, the variance analytically computed from the PCE coefficient is the same as obtained by Monte Carlo.

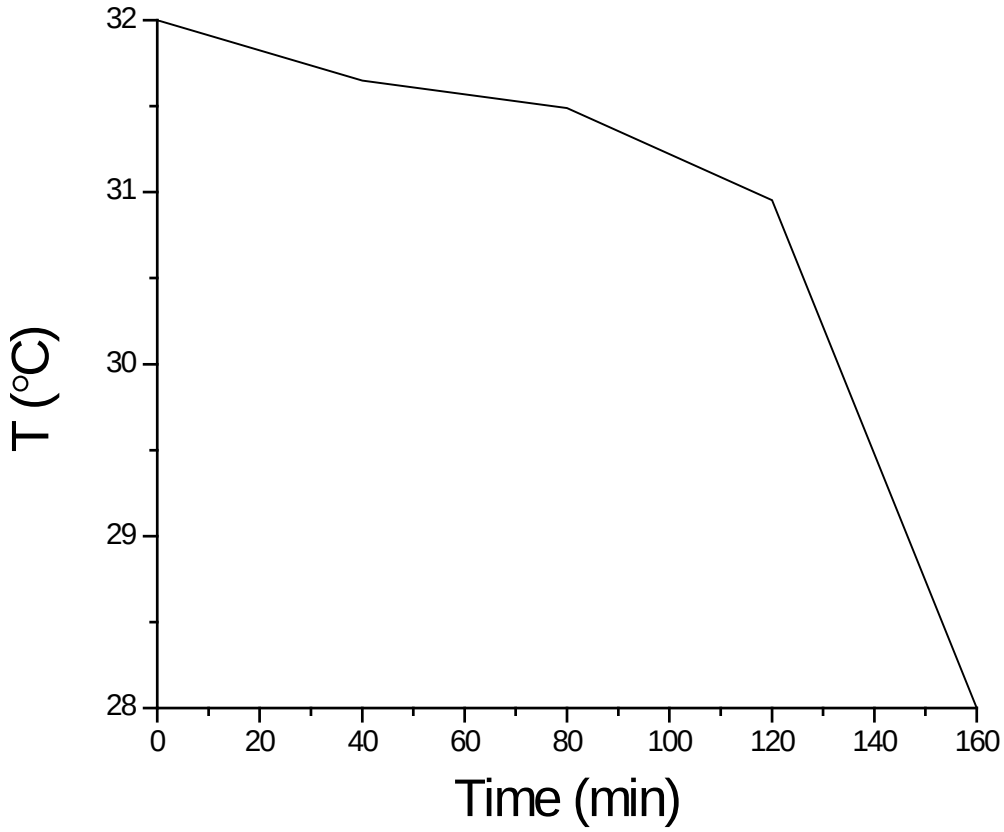

Fig. 6.1. Variant of optimal temperature profile for $J = J_{n.s.r.}$.

Table 6.1. Estimate of the variance from coefficients of the PCE for various standard deviations for the zeroth moment of the crystals in a batch crystallization process.

Standard Dev. of T (°C)	Estimate of Variance	Error
0.01	40279	13%
0.1	41988	9%
1.0	40106	13%

Table 6.2. Estimate of the variance from different schemes including from coefficients in the design of Li-ion batteries.

Scheme	Variance ($\times 10^6$)
Monte Carlo on full model	2.436
1st order series expansion	2.320
Monte Carlo on PCE	2.434
PCE coefficients	2.420

CHAPTER 7: CONCLUSIONS AND FUTURE WORK

7.1. Conclusions

Product performance can be improved by new process and materials chemistries as well as by the model-based optimal design. All models have associated uncertainties, and ignoring those uncertainties can largely reduce the increased performance obtained by model-based optimization. This thesis considers robust optimization techniques for producing designs that are optimal not just for nominal conditions but also in the presence of uncertainties.

This thesis considers the design of Li-ion batteries, motivated both by their existing market penetration and in their potential in new applications such as for the storage of energy generated by wind power. The robust optimization of Li-ion batteries with spatially-varying electrodes was investigated, in which it was found that an optimal spatial variation in porosity leads to enhanced robustness in the design. Increases in both nominal product performance and in robustness to variations that occur during manufacturing both motivate an experimental effort to manufacture such porous electrodes.

This thesis also proposed a new formulation for robust optimization based on polynomial chaos expansions, which incorporated analytically computed variances. This work considered two case studies: a well-studied batch crystallization process and a Li-ion battery. It was found that the analytical variance estimates were accurate enough for use in a multiobjective optimization for robust optimal design. The computational cost in the proposed approach is minimal because once the coefficients of the PCE are known,

the variance is computable almost for free. The robust optimization is also more tractable when the design variables are represented in the simple polynomial form.

7.2. Future Work

While acceptable for a case on robust optimization, the practical value of performing robust optimization for a Li-ion battery model with only one electrode being modeled in detail are minimal. A Li-ion battery model with a detailed description of all components would be more suitable for the robust optimal design of Li-ion batteries. The full advantages and machinery of robust optimization techniques would be more apparent for such a detailed model, as such as model would be more computationally expensive.

The new formulation for robust optimization proposed in this thesis should be applied to additional systems or processes, to demonstrate its broader utility. The mathematical formulation could be incorporated into existing robust optimization software packages such as in DAKOTA [17] or MATLAB.

REFERENCES

[1] R. Gunawan, M. Y. L. Jung, E. G. Seebauer and R. D. Braatz, "Optimal control of rapid thermal annealing in a semiconductor process," Journal of Process Control, 14 (2004) 423-430.

[2] V. Srinivasan and J. Newman, "Design and optimization of a natural graphite / iron phosphate lithium-ion cell," Journal of the Electrochemical Society, 151 (2004) A1530-A1538.

[3] J. Christensen, V. Srinivasan and J. Newman, "Optimization of lithium titanate electrodes for high-power cells," Journal of the Electrochemical Society, 153 (2006) A560-A565.

[4] V. Ramadesigan, R. N. Methekar, F. Latinwo, R. D. Braatz and V. R. Subramanian, "Optimal porosity distribution for minimized ohmic drop across a porous electrode," Journal of the Electrochemical Society, 157 (2010) A1328-A1334.

[5] Q. Hu, S. Rohani and A. Jutan, "Modeling and optimization of seeded batch crystallizers," Computers & Chemical Engineering, 29 (2005) 911-918.

[6] Q. Hu, S. Rohani, D. X. Wang and A. Jutan, "Optimal control of a batch cooling seeded crystallizer," Powder Technology, 156 (2005) 170-176.

[7] D. L. Ma and R. D. Braatz, "Robust identification and control of batch processes," Computers & Chemical Engineering, 27 (2003) 1175-1184.

[8] Z. K. Nagy and R. D. Braatz, "Robust nonlinear model predictive control of batch processes," AIChE Journal, 49 (2003) 1776-1786.

[9] Z. K. Nagy and R. D. Braatz, “Open-loop and closed-loop robust optimal control of batch processes using distributional and worst-case analysis,” Journal of Process Control, 14 (2004) 411-422.

[10] Z. K. Nagy and R. D. Braatz, “Worst-case and distributional robustness analysis of finite-time control trajectories for nonlinear distributed parameter systems,” IEEE Transaction on Control Systems Technology, 11 (2003) 694-704.

[11] Darlington, J., C.C. Pantelides, B. Rustem and B.A. Tanyi, “Decreasing the sensitivity of open-loop optimal solutions in decision making under uncertainty,” European Journal of Operations Research, 121 (2000) 343-362.

[12] Darlington, J., C.C. Pantelides, B. Rustem and B.A. Tanyi, “An algorithm for constrained nonlinear optimization under uncertainty,” Automatica, 35 (1999) 217-228.

[13] Z. K. Nagy and R. D. Braatz, “Distributional uncertainty analysis using power series and polynomial chaos expansions,” Journal of Process Control, 17 (2007) 229-240.

[14] S.S. Isukapalli, *Uncertainty Analysis of Transport-Transformation Models*, Ph.D. thesis, Rutgers University, New Brunswick, New Jersey, 1999.

[15] W. W. Pan, M. A. Tatang, G. J. McRae, and R. G. Prinn, “Uncertainty analysis of direct radiative forcing by anthropogenic sulfate aerosols,” Journal of Geophysical Research-Atmospheres, 102 (1997) 21915-21924.

[16] C. Wang, *Parametric Uncertainty Analysis of Complex Engineering Systems*, Ph.D. thesis, Massachusetts Institute of Technology, Cambridge, MA, 1999.

[17] B. M. Adams, W. J. Bohnhoff, K. R. Dalbey, J. P. Eddy, M. S. Eldred, D. M. Gay, K. Haskell, P. D. Hough and L. P. Swiler, *DAKOTA, A Multilevel Parallel Object-Oriented Framework for Design Optimization, Parameter Estimation, Uncertainty Quantification, and Sensitivity Analysis: Version 5.0 User's Manual*, Sandia Technical Report SAND2010-2183, December 2009.